Hindawi
Advances in Meteorology
Volume 2023, Article ID 5142965, 13 pages
https://doi.org/10.1155/2023/5142965

Research Article

Accuracy Evaluation of Standardized Precipitation Index (SPI) Estimation under Conventional Assumption in Yeşilırmak, Kızılırmak, and Konya Closed Basins, Turkey

Mehmet Ali Hinis[1] **and Mehmet Selim Geyikli**[2]

[1]*Department of Civil Engineering, Aksaray University, 68100 Aksaray, Turkey*
[2]*Department of Civil Engineering, Tokat Gaziosmanpasa University, 60250 Tokat, Turkey*

Correspondence should be addressed to Mehmet Ali Hinis; mhinis@gmail.com

Received 15 December 2022; Revised 23 March 2023; Accepted 30 March 2023; Published 17 April 2023

Academic Editor: Anzhen Qin

The doubt in the calculation algorithm of the standardized precipitation index (SPI), which is widely preferred in the evaluation and monitoring of drought, still remains up-to-date because its calculation process is performed in the form of standardization or normalization with a default probability distribution. Therefore, the success of this index is directly affected by the choice of the probability distribution model. This study is based on the effect of three different parameter estimation methods on the calculation process, as well as the comparison of the SPI results calculated based on the default Gamma distribution and the distribution with the best ability to represent the 3-and 12-month consecutive summed rainfall data among the 15 candidate distributions namely Gamma (GAM), Generalized Extreme Value (GEV), Pearson Type III (P III), Log Pearson Type III (LP III), two-parameter Lognormal (LN2), three-parameter Lognormal (LN3), Generalized Logistic (GLOG), Extreme Value Type I (EVI), Generalized Pareto (GPAR), Weilbul (W), Normal (N), Exponential (EXP), Logistic (LOG), four-parameter Wakeby (WK4), and five-parameter Wakeby (WK5) distributions. Approximately 68.4% and 18.4% of the 3-month data considered had the best fit to the Weibull and Pearson III distribution, while approximately 24% and 18% of the 12-month data had the best fit to the Weibull and Logistic distribution. On the other hand, it was found that the default Gamma distribution calculated the extreme drought categories significantly more than the best-fit distribution model. In terms of parameter estimation methods, L-moments for 3-month series and maximum likelihood approaches for 12-month series were most dominant.

1. Introduction

The fast expansion of technical advancements following the industrial revolution has led to excessive use of natural resources, in addition to human population growth, which is the primary reason of global ecosystem deteriorating. Since the middle of the 20th century, global warming has been the most significant and dangerous signal of human-oriented ecological disturbance [1]. This global threat, which emerged as a result of the increase in greenhouse gas emissions into the atmosphere, caused a serious increase in the earth's air temperature [2–4]. In the context of global warming, the normal functioning of the hydrological cycle has been disrupted, resulting in serious changes in the distribution and amount of rainfall on the earth. Natural catastrophes, including flooding, drought, and hurricane, have grown as a result of this unfavorable outcome; yet, major hazards have emerged in relation to water resources and agriculture [3, 5, 6]. This threat affecting the globe continues to manifest itself through extreme weather in different regions [7–10]. All components of the environment are negatively impacted by the drought, which results from a prolonged decrease in precipitation from normal levels. It also poses a major danger to the social and economic situations of humanity [11–13]. Characteristics such as the slow development of the drought and its continuation for many years caused this natural disaster to be regarded as the riskiest threat to

human and agriculture compared to other natural disasters experienced on a global scale [14].

The variability in climate in Turkey, especially in the context of precipitation and stream flow, has been revealed by various studies. During the dry season, the Mediterranean region, including Turkey, had a significant decrease in mean precipitation and an increase in precipitation variability, according to [15–17]. It has been discovered that there are changes in precipitation caused by the effects of global warming, especially in the eastern and southeastern portions of Turkey [18]. It has been observed that there are visible spatial and temporal variations in precipitation [19]. A trend study revealed a considerable decrease in precipitation, particularly in the winter [20], and a global climate model predicts major drops in annual streamflow and precipitation [21–23]. It was discovered that streamflows were significantly on the decline in the west and southwest of Turkey, [24] and in the middle of Turkey [25], the common opinion put forward in these studies is that there will be significant decreases in precipitation and streamflow, while an increase in precipitation is expected only along the Black Sea coast. Considering the detrimental consequences of climate change on Turkey's water supplies, it is obvious that the agricultural sector will be most severely impacted [26, 27]. Approximately 34.3% of Turkey's population is engaged in agricultural activities. On the other hand, 26.4% of 112 billion·m^3 (≈29.6 billion·m^3) of usable water potential in Turkey is used for irrigation [28].

It is conceivable that the typical process of moisture creation has been impacted by the phenomena of global climate change, particularly given its detrimental effects on temperature and precipitation. Therefore, this variation in moisture conditions will surely disturb the ecosystem's natural structure, especially with regard to concerns such as agriculture, water resources, and desertification. Wang [29] reported that fluctuation in moisture played a key role in analyzing drought conditions in a region. In terms of evapotranspiration, rainfall, soil moisture content, and groundwater, drought is a complex process [13]. Successfully defining and predicting drought, which is formed under the influence of many parameters that contribute to its emergence, is just considered difficult. In addition to drought prediction indicators such as the Reconnaissance Drought Index (RDI), Standardized Precipitation Evapotranspiration (SPEI), and Palmer Drought Severity Index (PDSI), which take into account many climate and soil-related parameters, there is also the widely used Standardized Precipitation Index (SPI) which defines drought with only one climate parameter, precipitation [7, 14, 30–32].

The SPI designed by McKee et al. [30] is based on the probability of precipitation time series at a given time scale. The SPI was set up for multiple time scales to determine the impact of drought on different water resources such as soil moisture, streamflow, groundwater, and reservoir storage. Rainfall deficiencies lasting 1 to 6 months give rise to meteorological and agricultural droughts, while exhausting or running dry of rivers, reservoirs, and groundwater due to precipitation deficiencies of up to 24 months or longer are associated with hydrological drought. The merit of this index compared to others is that only rainfall parameter is needed as input, and it can be easily calculated at different time scales. One of the obvious weaknesses of the SPI index is that it only quantifies the lack of precipitation [31, 32]. Another drawback is that at least 30 years' monthly rainfall data are required [33] for drought monitoring over a selected time period. Gutman [34] suggested that SPI calculation from 1 month up to 24 months was statistically sufficient. In the study of Edwards [35], the calculation process of SPI was based on the two-parameter Gamma distribution and the standard normal distribution whose mean value and standard deviation are zero and one, respectively. The assumption that the rainfall data to be subjected to the SPI calculation fit the two-parameter Gamma distribution was related to the finding of Thom [36], who reported that rainfall series followed the Gamma distribution well. In fact, this assumption is most widely used in SPI-based drought monitoring models in the literature. Although there is a generalization that the rainfall data fit the Gamma distribution well, the differences in the occurrence conditions of this climatic event are dependent upon their frequency distribution characteristics. For this reason, there would always be a doubt in the SPI calculations based on the assumption. Moreover, some researchers [37–40] expressed the inadequacy of the Gamma distribution originally suggested by McKee et al. [30]. For the more reasonable analysis of drought with the SPI, the preference of the Pearson Type III distribution, which was the three-parameter version of the two-parameter Gamma distribution, approach, recommended by Guttman [34], was also criticized [37, 39]. In this context, it is important for reliable decisions to determine the theoretical distribution that could best represent the data to be analyzed in the monitoring and evaluation of the drought levels in a given region, based on SPI. However, some researchers have taken into account a limited number of theoretical distributions for the studied region data in the SPI calculation. Yılmaz et al. [41] used Normal, Lognormal, Gamma, Logistic, Log-logistic, and Weibull distributions to determine the distribution suitable for the data in the study area while describing the meteorological drought in the upper Coruh basin. Mahmoudi et al. [42] highlighted that the generalized extreme value distribution at different time scales was a more accurate alternative for the SPI calculation compared to the default Gamma distribution. Pieper et al. [43] argued for the use of exponentiated Weibull distribution when calculating SPI, instead of the default Gamma distribution.

The drawbacks outlined above in the use of the SPI in monitoring and evaluation of drought still remain up-to-date before being a reasonable index, and these distribution models should be well evaluated in the context of making successful decisions. From this perspective, it becomes very crucial to select the favorite probability distribution model to be used in the SPI calculation process. The purpose of this study was to identify the best suitable theoretical probability distribution for rainfall data in the phase of drought monitoring and assessment using the SPI calculation method in three basins in Turkey with various meteorological features. While making this attempt, many

parameter estimate approaches have been incorporated into the scenario. The attempt was made to identify the differences between the SPI values calculated using the frequently used default Gamma distribution and the closest distribution to the supplied data.

The rest of the paper is organized as follows. Description of the study area is given in Section 2.1, methodology is given in Section 2. The results are presented in Section 3, discussion is provided in Section 3.2, and concluding remarks are provided in Section 4.

2. Research Methodology/Research Design

2.1. Description of the Study Area. The study area includes three catchment basins in Turkey, where different climatic types are experienced, namely Yeşilırmak, Kızılırmak, and Konya Closed Basins. Yeşilırmak River is the second longest river in Turkey with a length of 519 km and has three main tributaries, namely Çekerek, Kelkit, and Tersakan. The river originates within the borders of Sivas province, and its flow finally ends in the Black Sea. The basin area is about 36114 km^2 (about 5% of Turkey's surface area) and the average annual precipitation is 528 mm. The Black Sea climate is dominant in the parts of the basin close to the Black Sea coast, and the continental climate is dominant in the inner regions. Black sea coast experiences a humid subtropical climate, with abundant precipitation, warm winters, and humid summers. It is under the influence of polar continental air accompanied by strong northeasterly winds, and frequent precipitation in winter. The average temperature of the basin is around 12°C [44]. The Kızılırmak River, which has a length of 1151 kilometers, is Turkey's longest river and corresponds to 11% of Turkey's surface area in terms of the area it covers. The basin is located between Yeşilirmak and Konya Closed Basins with its geographical location. The annual average precipitation and temperature of the basin are 445 mm and 13.7°C. The Kızılırmak River, similar to the Yeşilırmak River, originates within the borders of Sivas province and drains into the Black Sea in Bafra district of Samsun province. Although the continental climate is experienced in the majority of the basin, the Black Sea climate is dominant in its parts close to the Black Sea. The distribution of precipitation in the basin varies considerably, which is 334.1 mm in Niğde and 781.7 mm in Bafra [25]. Konya Closed Basin covers an area of 53850 km^2 (approximately 7% of Turkey's surface area). The annual average total precipitation in the basin was recorded between 286 mm (Karapınar) and 740 mm (Seydişehir). When the precipitation observed in Seydişehir is excluded, the regional average of precipitation is around 345 mm. This basin includes the area (around Salt Lake) where precipitation occurs the least in Turkey. The basin which is a dominant continental climate has arid and semiarid characteristics with low precipitation and high evaporation [45].

In the study, the monthly rainfall data measured between 1975 and 2020 at the precipitation stations operated by the General Directorate of State Meteorology Affairs in the basins in question were used as input data. For the study, 38 rainfall stations with at least 30 years of continuous precipitation data were included in the study (Table 1). Figure 1 shows the geographic locations of stations in the three basins. Missing data at stations were completed with the linear regression approach.

2.2. Datasets

2.2.1. Standardized Precipitation Index (SPI) Calculation Algorithm. As it is well known, the original SPI calculation technique involves fitting data to a standardized normal distribution with a mean of zero and a variance of one by subtracting the mean of the series from each value of the rainfall series and dividing the difference by the series' standard deviation [30]. Therefore, each calculated Z-value represents the SPI value. However, performing the calculation from the SPI original relationship is only possible by confirming the data is normally distributed. Considering that the hydrometeorological data are generally not approximately normally distributed, the SPI calculation process is mostly realized based on an alternative distribution, namely the two-parameter Gamma distribution [46]. This presupposition-based SPI calculation process was described in detail by Edwards [35]. The SPI calculation algorithm is formulated in the following relationship over a distribution that most approximately fits the data studied:

$$\mathrm{SPI} = \Phi^{-1}\left[F_{\mathrm{CDF}}\left(x_t\right)\right], \tag{1}$$

where x_t is the observed or consecutive summed rainfall for the considered time scale (t); F_{CDF} is the cumulative probability distribution; and Φ^{-1} is the inverse of the standard normal distribution, also named z-distribution, with zero mean and one variance. Drought classes were tabulated based on SPI (Table 2) [30].

In this study, the theoretical probability distribution models presented in Table 3 were applied to the rainfall data formed by sequentially summing for different time scales (3-month and 12-month) in order to remove the concern about the two-parameter Gamma distribution, which is widely accepted in the SPI calculation algorithm. In addition, the parameters of the considered distribution models were estimated by the method of moments (M), maximum likelihood (ML), and L-moments (LM). The distribution model that most approximates the available data was also chosen based on the Kolmogorov–Smirnov test [47]. By comparing the distributions of the two datasets, the Kolmogorov–Smirnov test is used to determine whether probability distributions are appropriate for the series. The null hypothesis (Ho) is that the two dataset values are from the same continuous distribution. The alternative hypothesis (Ha) is that these two datasets are from different continuous distributions. The hypothesis test can be carried out at a specific statistical significance level (e.g., 5% taken is this study). If the calculated values of the KS test statistic are lower than those of the theoretical values at the chosen significance level, then the model distribution is taken to be acceptable for estimation. The three distinct parameter estimation techniques (M, ML, and LM) utilized to derive the parameters of the 15 theoretical probability distributions given

Table 1: Some features of the rainfall stations in the study area.

Basin		Rainfall station	Longitude (E)	Latitude (N)	Elevation (meter)	Observation period	Mean (mm)
Yeşilirmak	1	Samsun	36°15′	41°21′	4	1975–2020	703.2
	2	Merzifon	35°27′	40°53′	754	1975–2012	439.5
	3	Corum	34°56′	40°32′	776	1975–2020	453.1
	4	Amasya	35°50′	40°40′	409	1975–2020	463.4
	5	Tokat	36°33′	40°20′	611	1975–2020	442.3
	6	Zile	35°53′	40°18′	719	1984–2020	444.7
	7	Sebinkarahisar	38°25′	40°17′	1364	1984–2020	436.5
	8	Turhal	36°06′	40°23′	528	1984–2020	413.1
	9	Susehri	38°04′	40°10′	1164	1985–2020	566.1
Kızılırmak	10	Kastamonu	33°47′	41°22′	800	1975–2020	511.3
	11	Cankiri	33°37′	40°36′	755	1975–2020	420.2
	12	Sivas	37°00′	39°45′	1294	1975–2020	455.4
	13	Kirikkale	33°31′	39°51′	751	1975–2020	390.2
	14	Yozgat	34°49′	39°50′	1301	1975–2020	604.5
	15	Kırsehir	34°09′	39°10′	1007	1975–2020	393.1
	16	Gemerek	36°05′	39°11′	1182	1975–2020	417.2
	17	Nevsehir	34°42′	38°37′	1260	1975–2020	429.2
	18	Kayseri	35°30′	38°41′	1094	1975–2020	410.6
	19	Bafra	35°55′	41°33′	103	1990–2020	487.7
	20	Ilgaz	33°38′	40°55′	885	1985–2020	340.3
	21	Tosya	34°02′	41°01′	870	1983–2020	464.2
	22	Osmancik	34°48′	40°59′	419	1984–2020	415.6
	23	Zara	37°44′	39°53′	1338	1985–2020	500.4
	24	Keskin	33°37′	39°40′	1140	1986–2020	409.0
	25	Cicekdagi	34°25′	39°36′	900	1984–2020	355.9
	26	Kaman	33°42′	39°22′	1075	1975–2020	469.1
	27	Bogazliyan	35°15′	39°12′	1070	1975–2020	367.9
	27	Urgup	34°55′	38°37′	1068	1975–2020	370.9
	29	Develi	35°29′	38°22′	1204	1975–2020	370.6
Konya Closed	30	Konya	32°34′	37°59′	1031	1975–2020	336.1
	31	Karaman	33°13′	37°12′	1018	1975–2020	348.0
	32	Eregli	34°03′	37°32′	1046	1975–2020	312.4
	33	Nigde	34°41′	37°57′	1211	1975–2020	347.6
	34	Kulu	33°04′	39°05′	1005	1975–2020	388.0
	35	Seydişehir	31°21′	38°04′	1158	1975–2020	772.3
	36	Cumra	32°47′	37°34′	1014	1975–2020	330.3
	37	Karapinar	33°32′	37°43′	996	1975–2020	307.1
	38	Aksaray	34°00′	38°22′	970	1975–2020	358.4

in Table 3. Theoretical probability distributions used in this study are Gamma (GAM), Generalized Extreme Value (GEV), Pearson Type III (P III), Log Pearson Type III (LP III), two-parameter Lognormal (LN2), three "-parameter Lognormal (LN3), Generalized Logistic (GLOG), Extreme Value Type I (EVI), Generalized Pareto (GPAR), Weibull (W), Normal (N), Exponential (EXP), Logistic (LOG), four-parameter Wakeby (WK4), and five-parameter Wakeby (WK5) distributions. Detailed information about these distributions and the estimation of their parameters by moments, maximum likelihood and L-moment techniques can be found in [48].

Among the candidate distributions, the one that most closely follows the data is determined by the following relationship based on the Kolmogorov–Smirnov approach. For this purpose, the nonexceedance probability (F_i) for each observation (x_i) of the existing data sorted in ascending order is calculated with a plotting position formula, and at the same time, the probability (F_i^{DIST}) of the observation in question in the considered theoretical distribution is also estimated. The Kolmogorov–Smirnov test statistic Δ is given in the following equation:

$$\Delta = \mathrm{Max}\left|F_i^{\mathrm{DIST}} - F_i\right|. \quad (2)$$

In equation (2), DIST corresponds to the candidate theoretical distribution. The critical value of the Δ_{cr} for a given significance value (i.e., 5% for this study) is compared. If $\Delta < \Delta_{cr}$, then the null hypothesis that the given distribution is a good fit is accepted, otherwise null hypothesis is rejected. If there are more than one value less than "Δ_cr" in the theoretical distributions considered, it is decided that the theoretical distribution with the smallest "Δ" value follows the data most closely and is the most appropriate distribution.

This methodological approach would provide the opportunity to judge the confusion that occupies the minds on the Gamma distribution. For this purpose, in addition to being analyzed statistically to determine the difference between the 3-month SPI and 12-month SPI series, which are

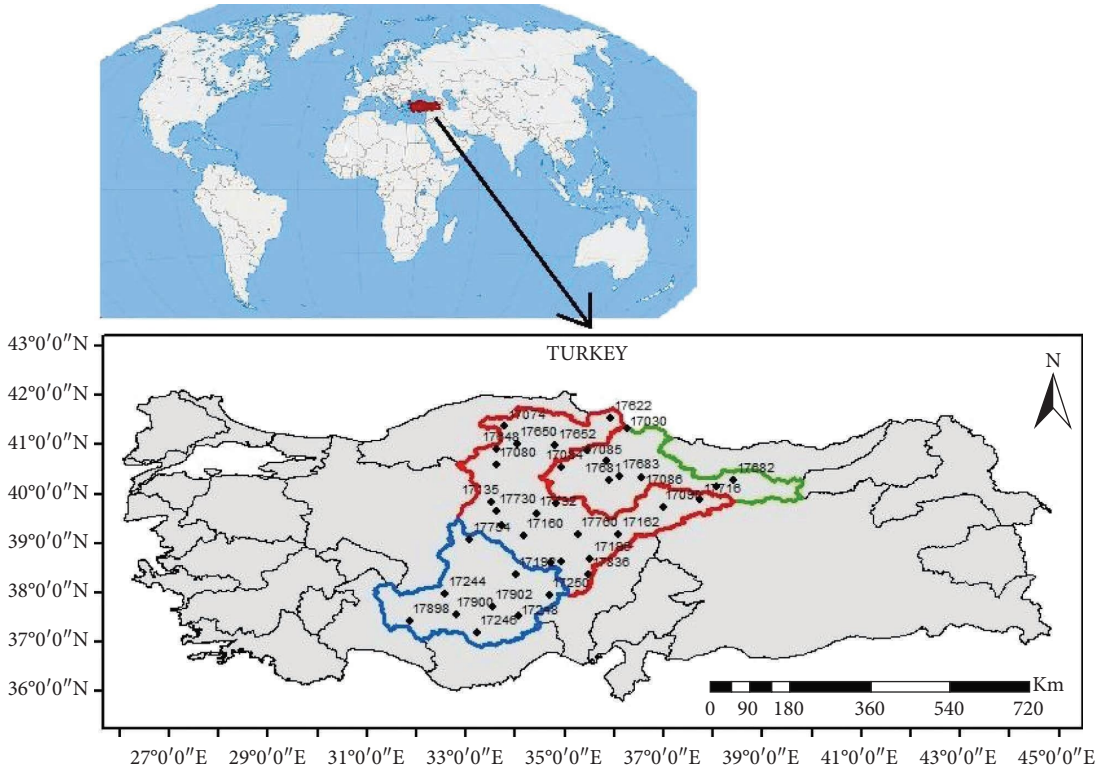

Figure 1: Study area and stations: Yeşilırmak Basin, Kızılırmak Basin, and Konya Closed Basin (shown as within the green, red, and blue boundaries, respectively).

Table 2: Drought classes based on SPI values.

SPI	SPI category	Abbreviation
>2	Extremely wet	EW
1.5 to 1.99	Very wet	VW
1.0 to 1.49	Moderately wet	MW
−0.99 to 0.99	Near normal	NN
−1.0 to −1.49	Moderately dry	MD
−1.5 to −1.99	Severely dry	SD
<−2	Extremely dry	ED

Table 3: Theoretical probability distribution models considered in the study.

Distributions (dist.)	Parameter estimation approaches (PEA)		
	Maximum likelihood (ML)	Moments (M)	L-moments (LM)
Generalized Extreme Value (GEV)	✓	✓	✓
Pearson Type III (P III)	✓	✓	✓
Three-parameter Lognormal (LN3)	✓	✓	✓
Generalized Logistic (GLOG)	✓	✓	✓
Extreme Value Type I (EVI)	✓	✓	✓
Generalized Pareto (GPAR)	✓	✓	✓
Weibull (W)	✓	✓	✓
Normal (N)	✓	✓	✓
Exponential (EXP)	✓	✓	✓
Logistic (LOG)	✓	✓	✓
Two-parameter Lognormal (LN2)	✓	✓	✓
Gamma (GAM)	✓	✓	✓
Log Pearson Type III (LP III)	✓	✓	✓
Four-parameter Wakeby (WK4)	—	—	✓
Five-parameter Wakeby (WK5)	—	—	✓

calculated based on the Gamma distribution and the theoretical distribution that most closely fits the data, the areal changes of these two series were also revealed on the basis of the studied area. Calculations and statistical analysis were carried out by Excel spreadsheet software, and ArcGIS software was used to plot the figures.

3. Results

The main aim of this study was to detect the difference between the SPI (Standardized Precipitation Index) values dealing with the consecutively summed rainfall series for 3-month and 12-month belonging to 38 precipitation stations, which were calculated based on the default Gamma distribution and theoretical probability distribution that most approximately fit the studied data. Therefore, first of all, among the theoretical distributions in Table 3, the distribution that best fits the formed rainfall data by sequentially summing for the 3-month and 12-month time scales was selected based on the Kolmogorov–Smirnov method. In Table 4, the most suitable probability distribution model for two data sets of each station and the parameter estimation approach (PEA) are presented. As can be seen from Table 4, 26 of 38 stations belonging to 3-month precipitation data are closest to the Weibull (W) distribution model. On the other hand, Pearson III (P III) model in the data of seven stations and Generalized Extreme Value (GEV) model in the data of two stations were found to be the most appropriate distributions. Surprisingly, the 3-month data of only one station provided the best fit for the two-parameter Gamma, two-parameter Lognormal, and three-parameter Lognormal models. Among the parameter estimation methods considered, the L-moments approach had a clear advantage in being preferred over the other two. The L-moment method came to the fore in 21 rainfall data.

For the 12-month time scale, the rainfall series of the stations in the study provided the best fit with the W and LOG distribution models at 9 and 7 stations, respectively. In addition, each of the N, LN 3, and GAM theoretical probability distributions showed the most approximate fit to the data of the four stations, whereas the LN 2 distribution model achieved the most successful fit at three stations, and the P III, GLOG, and GEV distribution models at two stations. The EVI theoretical probability distribution model also showed the most approximate fit for only one station data. These findings indicated that the 12-month rainfall data of 38 stations showed more frequency distribution characteristics than the 3-month rainfall data. While the maximum likelihood parameter estimation method was more accepted than the moment and L-moments methods, the remaining other two approaches could not outcompete each other in almost all cases. In fact, these findings provided for both time scales were explicit proof that how much the concern over SPI values calculated based on the default Gamma model was justified. Although the Weibull model approved to be the most suitable for the time scales in question was more preferred than the others, the six and ten separate distribution models for the rainfall data sets of the 3-month and the 12-months, respectively, showed the most approximate fit. Therefore, instead of performing the SPI calculation algorithm with the Gamma model based on the finding of [36], it would be more realistic to reach reliable results by including the distribution model that best fits the data studied and even the parameter estimation method.

Table 4: Theoretical distribution models most approximately fitting the rainfall data of 3-month and 12-month for the sites.

Rainfall station	Dist. 3-month	PEA	Dist. 12-month	PEA
Samsun	P III	ML	N	ML
Merzifon	W	ML	LN 3	ML
Corum	W	LM	P III	ML
Amasya	W	LM	LN 3	M
Tokat	W	LM	W	M
Zile	W	LM	GAM	LM
Sebinkarahisar	W	M	LOG	ML
Turhal	W	LM	LOG	ML
Susehri	W	LM	N	ML
Kastamonu	LN 2	LM	LN 2	ML
Cankiri	P III	M	N	ML
Sivas	P III	M	N	LM
Kirikkale	W	LM	LOG	ML
Yozgat	W	LM	GAM	ML
Kırsehir	W	M	GAM	M
Gemerek	W	LM	LOG	LM
Nevsehir	W	LM	GAM	LM
Kayseri	W	LM	LOG	LM
Bafra	P III	ML	LN 2	ML
Ilgaz	W	LM	W	M
Tosya	GEV	M	W	LM
Osmancik	P III	ML	W	M
Zara	W	M	LOG	LM
Keskin	W	LM	LN 3	ML
Cicekdagi	W	LM	EV I	M
Kaman	W	M	W	M
Bogazliyan	GEV	LM	LOG	ML
Urgup	W	LM	W	LM
Develi	LN 3	ML	GLOG	ML
Konya	P III	ML	W	LM
Karaman	P III	ML	P III	ML
Eregli	W	M	W	M
Nigde	W	LM	LN 3	ML
Kulu	W	LM	GEV	M
Seydişehir	GAM	ML	GLOG	ML
Cumra	W	M	W	M
Karapinar	W	LM	LN 2	LM
Aksaray	W	LM	GEV	M

*Abbreviations of distributions used in this study: W: Weibull; P III: Pearson Type III; GEV: Generalized Extreme Value; GAM: Gamma; LN2: two-parameter Lognormal, LN3: three-parameter Lognormal; N: Normal; LOG: Logistic; GLOG: Generalized Logistic; EVI: Extreme Value Type1.

The comparison of the results of each SPI-drought category calculated based on the best-fitted distribution model selected for the considered data and the Gamma distribution model are presented in Figure 2. For SPI-3 at the stations in the study area, it was found that the extreme drought and extreme wet categories, abbreviated as EW and ED, were experienced remarkably more in the most suitable theoretical distribution model and Gamma model, respectively. Moreover, the lead in this difference was more pronounced in the ED drought category. Therefore, the

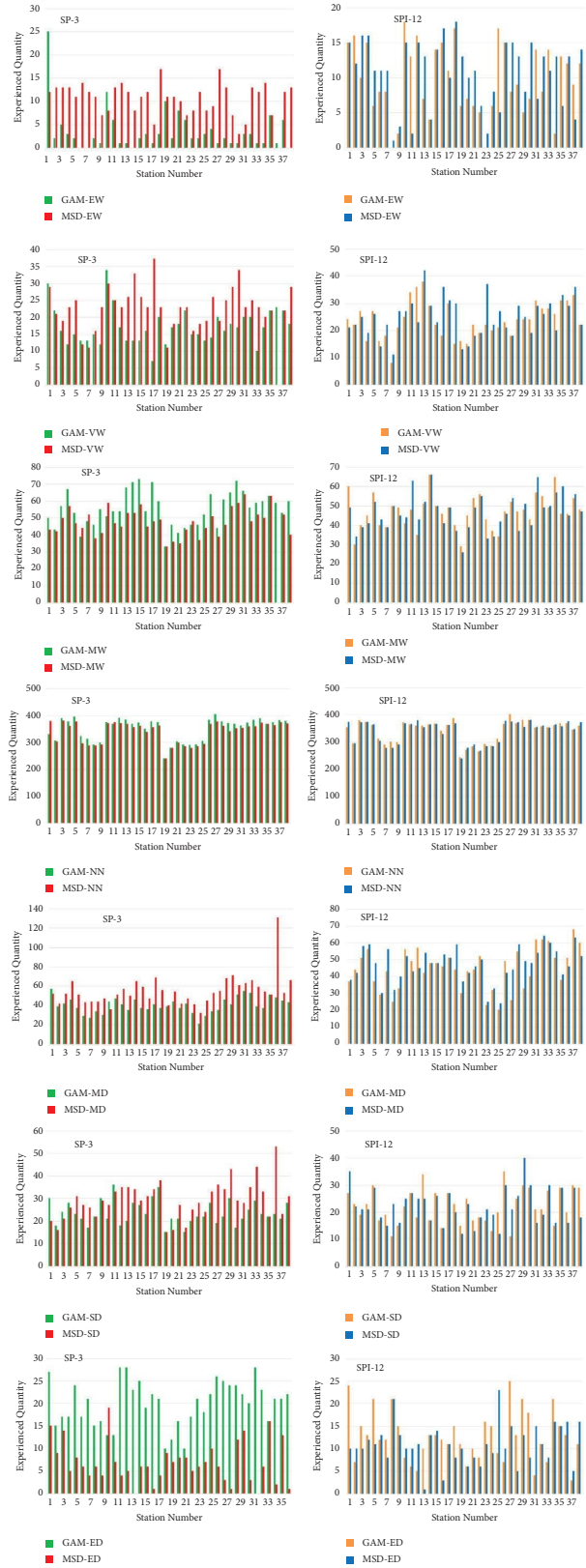

Figure 2: Comparison of SPI3 and SPI12 drought categories calculated based on Gamma distribution and Most Suitable distribution.

Gamma probability distribution model has detected a much greater number of dry periods. The fact that serious attention should be paid to the correctness of making projections for the future (especially in the decisions made on agricultural drought) with results based on Gamma distribution should be brought to the agenda by the addressees of the subject again. The MD drought category became numerically higher in almost all stations (except Samsun and Kastamonu stations) based on the best-fit distribution model. The SD drought category was predicted in greater numbers at six stations with the Gamma distribution model.

The ED drought category for SPI-12 was numerically determined more in the Gamma model as it was for SPI-3. However, this numerical superiority was not evident compared to SPI-3. On the other hand, when all the remaining drought categories were evaluated one-by-one, a clear difference could not be detected between the results provided from the best-fit distribution model and the Gamma model. However, it is obvious that there is a partial advantage over the Gamma distribution with the most appropriate distribution model. Similar results were also obtained in the 12-month rainfall series, although not as pronounced as in the 3-month rainfall series. Spatial variability of the best-fit probability distributions over the study area is given in Figure 3.

Table 5 shows the percentiles of the best distributions in the study area for the SPI 3 and SPI 12 drought calculations. The Weibull distribution was the dominant distribution for SPI 3, dominating 68.42% of the entire study area. The P-3 distribution was the second most used distribution with an area of 18.42%, and the GEV distribution was the third most used distribution with a 5.26% area. While GAM, LN-2, and LN-3 were the least common distributions with a usage area of 2.63%, LOG, NORM, and EV-1 distributions were not found in any area as the most appropriate distribution. On the other hand, in the SPI 12 drought calculation, the dominant best distribution was the Weibull distribution with a rate of 23.68% in the study area, as in the SPI 3 calculation. The LOG distribution, which is not seen in the SPI 3 calculation, took the second place as the best distribution in an area of 18.42%. This was followed by LN-3 distribution with 13.16%, GAM and NORM with 10.53%. P-3, GEV, GLOG, and LN2 distributions were seen in an area of 5.26%, and the least common distribution was EV1 with 2.63%. In the SPI3 and SPI12 drought calculations, although different distributions emerged as the best distribution on an aerial basis, the Weibull distribution appears to be the most appropriate distribution in common.

Comparison of the results of SPI3 and SPI12 droughts based on the Gamma distribution and Most Suitable Distribution for selected times is given in Figure 4. The spatial distribution of the SPI 3 drought in October 1993 for the investigated basins is given in Figure 4(a) for the Gamma distribution and in Figure 4(b) for the Most Suitable Distribution. When these two graphs are examined, it is seen that there is a clear difference between the dry and wet regions in the areal distribution due to the difference in the calculation method. In the calculations made with the MSD method, it is seen that more areas are affected by drought compared to the Gamma method. While the areas falling into the ED, SD, and MD classes were 13.2%, 7.9%, and 7.9% for the Gamma distribution; for MSD, it was 23.7%, 26.3%, and 15.8%, respectively. In wetlands, the classes with EW, VW, and MW were 5.3%, 0%, and 2.6% when calculated by the Gamma distribution, while these classes were found to be 2.6%, 2.6%, and 0% when calculated by the MSD method.

SPI12 calculations for the period of September 2012 are given in Figure 4(c) for the Gamma distribution and in Figure 4(d) for the MSD method. In this period, it was found that more areas were in drought classification in the MSD method (%31.6) compared to the Gamma method (%18.4). For ED, SD, and MD drought classes, the areas of the basins examined in the Gamma method were 2.6%, 10.5%, and 5.3%, while these areas were 15.8%, 7.9%, and 7.9% in the MSD method, respectively.

According to the Gamma distribution, it was observed that the total area in the wet period was higher than that calculated by MSD. While the areal percentages were 5.3%, 7.9%, and 13.1% in the calculations made according to the Gamma method for the EW, VW, and MW classes; these areas were found to be 5.3%, 5.3%, and 5.3% in the MSD method, respectively. It was found that more areas (%26.3) are in the Wet period in the Gamma distribution method compared to the MSD method (% 15.8).

4. Discussion

The basis for reliable SPI calculation depends on choosing an appropriate probability distribution for precipitation. McKee et al. [30] proposed SPI and assumed that cumulative precipitation follows a Gamma distribution (GAM). In many parts of the world, the gamma distribution has been chosen and found to be suitable for SPI computation, including Stagge et al. [39] for Europe, Okpara et al. [49] for West Africa, Blain et al. [50] for Brazil, and Zhao et al. [51] for China.

Various distributions, including various types and parameters of probability distributions, would result in various SPI values. Guttman [34] suggested Pearson Type III distribution for SPI calculations for the United States. Sienz et al. [32] showed that the Weibull-type distribution fits the monthly precipitation in Europe much better than the Gamma distribution. Pieper et al. [43] recommended the exponential Weibull distribution as the basis for SPI calculations. Wang et al. [52] investigated five candidate distributions to describe cumulative precipitation series for SPI analysis for China. They concluded the Gamma distribution is the optimal choice for calculating SPI with time scales from 1 month to 12 month in China among the five candidate distributions namely Gamma, Weibull, Generalized Extreme Value, Pearson Type III, and Tweedie distributions. They stated that the uncertainty in the SPI calculation decreased with the increase of the time scale and recording length, mainly as a result of the decrease in the confidence interval width of the Gamma distribution parameters.

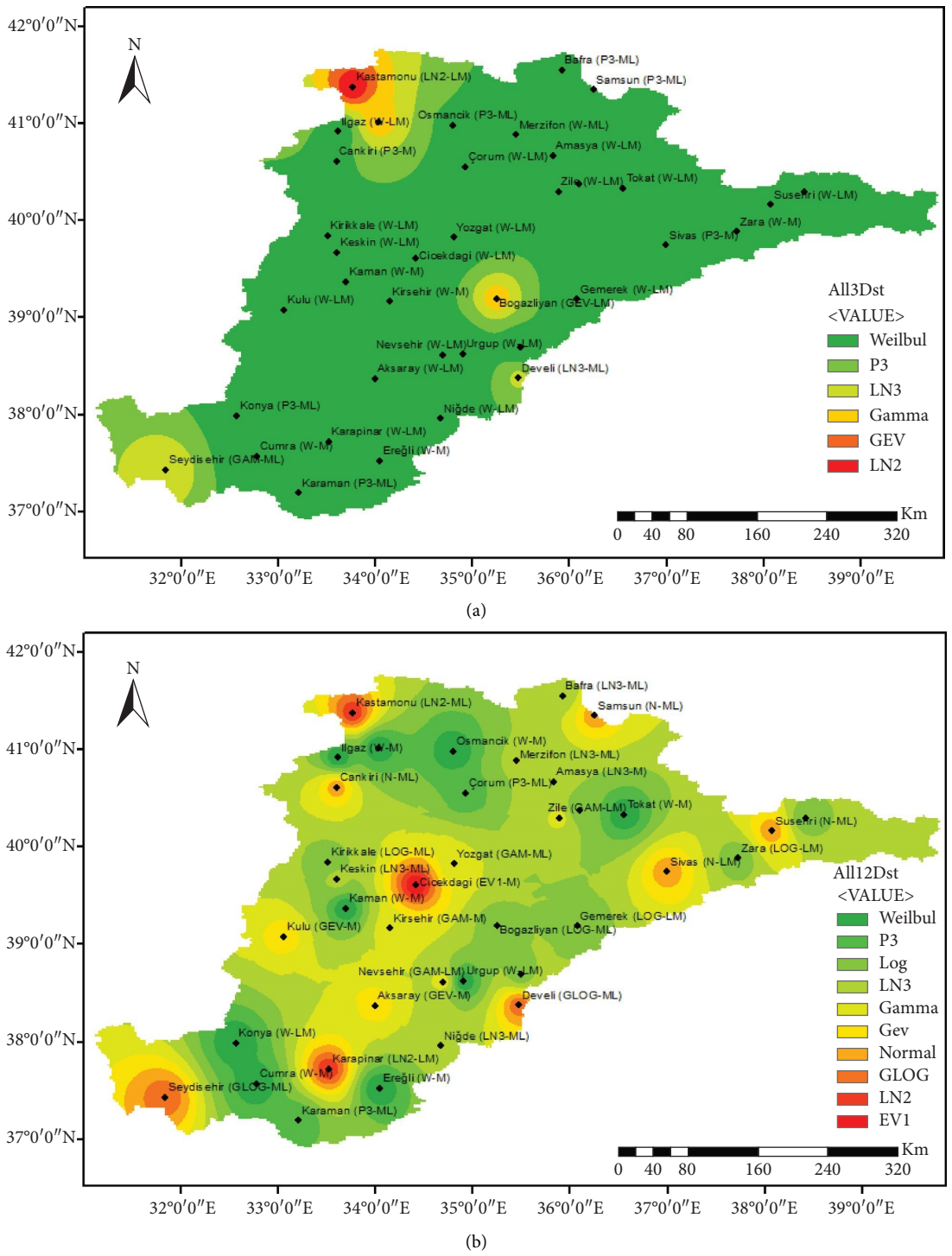

Figure 3: Spatial variability of the best-fit probability distribution models observed in the study region for (a) SPI3 and (b) SPI 12 drought calculations.

Kömüşçü et al. [53] investigated the drought climatology of Turkey by applying SPI and found that drought events paint a diverse but consistent picture with varying timescales, such as severe droughts occurring in shorter time periods typical of the interior of the country. Sonmez et al. [54] used SPI to investigate Turkey's vulnerability to meteorological drought. They discovered that for SPI 3 mild droughts occurred frequently in short time steps and for SPI 12 moderate droughts occurred more frequently and affected roughly two-thirds of the country. For SPI12, there have been less documented severe droughts. The inferences of Sonmez et al. [54] coincides with the result of the present study.

In dry and semiarid regions, Mahmoudi et al. [42] intended to modify the SPI calculating procedure. They

Table 5: Areal percentage of the best fit distributions given in Figure 3.

Probability distribution	Area for SPI 3 (%)	Area for SPI 12 (%)
Weibull	68.42	23.68
P-3	18.42	5.26
LOG	0	18.42
LN-3	2.63	13.16
GAM	2.63	10.53
GEV	5.26	5.26
NORM	0	10.53
GLOG	0	5.26
LN-2	2.63	5.26
EV1	0	2.63

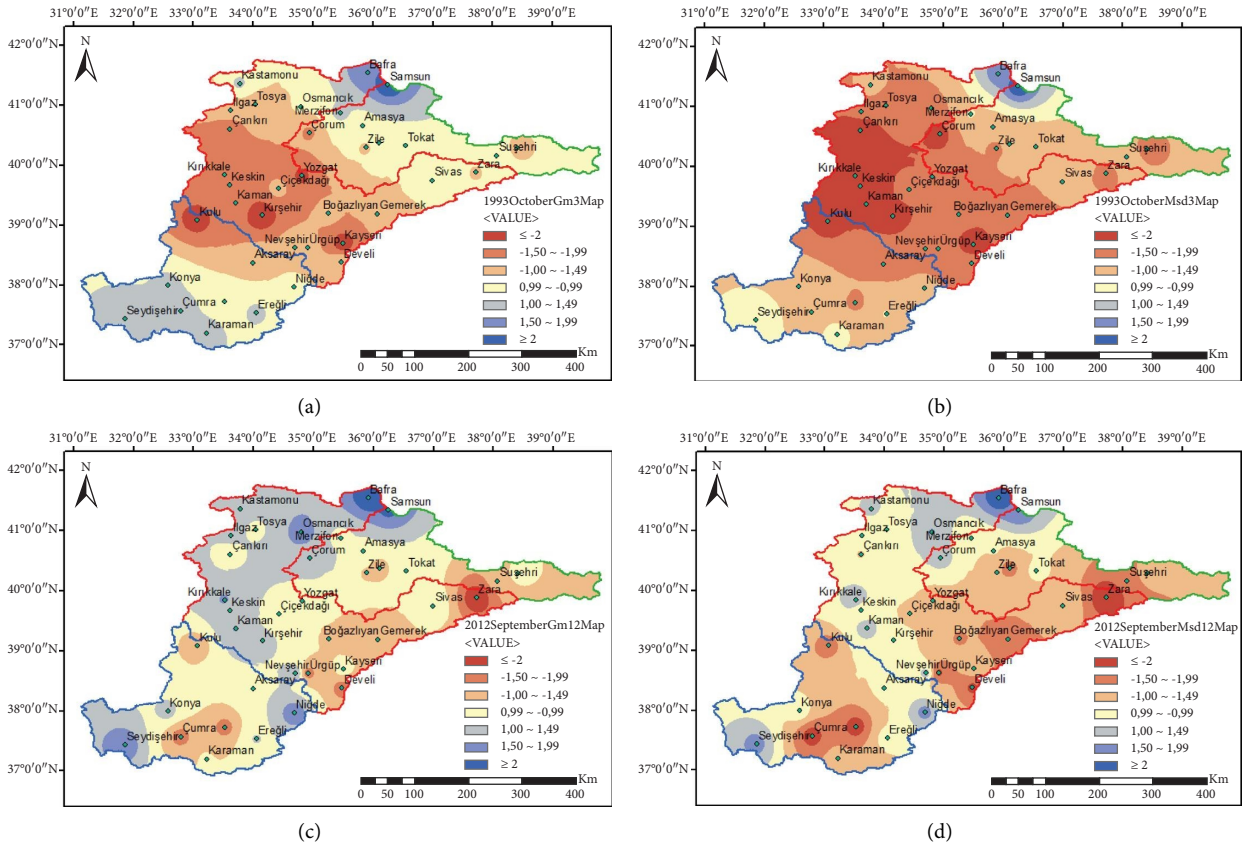

Figure 4: Comparison of spatial distributions of SPI3 and SPI12 drought calculations according to Gamma distribution and most suitable distributions (MSD) for selected months: (a) SPI3 with Gamma for October 1993, (b) SPI 3 with MSD for October 1993, (c) SPI 12 with Gamma for September 2012, and (d) SPI12 with MSD for September 2012.

came to the conclusion that there was no single distribution function that could be recommended as a workable replacement for the Gamma distribution for calculating the Standardized Precipitation Index (SPI) at various time scales, so they each proposed a different distribution for a particular time period.

Weibull and Pearson Type III distributions (68.42% and 18.42% as areal distributions) were found to be the most suitable distributions in this study for SPI 3; Weibull and Logistic distributions (23.68% and 18.42% as areal distributions) were found to be the most suitable distribution for SPI12. On the other hand, it was discovered that the default Gamma distribution was the most appropriate distribution, accounting for just 2.63% of the total area for SPI3 and 10.53% for SPI12. The goodness-of-fit results for the 3-and 12-month precipitation series indicate that using Thom's [36] advice for SPI calculations may not produce the best results. Similar results were reported by Akturk et al. [55] for the Pearson Type III distribution, which was determined to be the second most acceptable distribution in the findings of the present study. Akturk et al. [55] used the Normal, Lognormal, two-parameter Gamma, and Pearson Type III

probability distributions in the research of the most appropriate probability distributions in the drought analysis of the Kızılırmak Basin; they came to the conclusion that the Pearson Type III probability distribution is the most suitable distribution for monthly precipitation in the majority of the stations.

In light of all of these findings, it is important to underline that the theoretical probability distribution model that can best describe the data in accordance with the conditions of each location should be used to develop an effective SPI drought forecast.

5. Conclusion

Drought, which is one of the most important natural disasters affecting our globe in terms of both the frequency of its experience and its area of influence, has considerable damage to water resources, agriculture, and the economy. In fact, it is predicted that the severity and duration of the natural dry processes experienced in some parts of our globe would increase further with the effect of global climate change, and even new places would be added to these areas. It is estimated that the southern and central regions of Turkey would also be under the influence of drought. This study was conducted over determining the theoretical probability distribution models that most approximately follow the 3- and 12-month series formed by sequentially summing the precipitations of three different basins in Turkey, the climate structure of which is different from each other. And then, Standardized Precipitation Index (SPI) results calculated using the distribution model chosen for each series were compared with those of the traditionally accepted two-parameter Gamma distribution. In addition to the selection of the theoretical distribution model, which has the ability to best represent the existing data, the effects of the use of three different approaches in the estimation of the parameters of the models on the results were also examined.

Approximately 68.4%, 18.4%, and 5.26% of the 3-month summed rainfall series formed with the rainfall data of 38 rainfall stations in the study area provided the most approximate fit to the Weibull, Pearson Type III, and Generalized Extreme Value distributions, respectively. Surprisingly, the default Gamma and the two- and three-parameter Lognormal distribution models showed the best fit at only one station. On the other hand, the rainfall series generated for a 12-month time period produced the best fit to the Weibull and Logistic distribution models at approximately 24% and 18% of the stations considered, respectively. The default Gamma distribution, on the other hand, had the ability to best represent the rainfall series created at four stations. Based on the goodness-of-fit results of the 3- and 12-month rainfall series, it could be expressed that making SPI calculations with Thom's [36] suggestion obviously leads to questionable results. Moreover, the 3-month rainfall series gave the best fit for only six of the candidate distributions considered, while the 12-month rainfall series provided the best fit for the ten theoretical distributions. This finding underlines that the frequency distribution shapes of the 12-month rainfall series are more variable than those of the 3-month rainfall series in the studied region.

For the 3-month series, the extreme drought category based on the SPI was experienced significantly more with the default Gamma distribution than that calculated from the best-fitted distribution model. However, the opposite situation turned in favor of the best-fitted distribution model in the extreme wet drought category. In fact, this result explains that more severe dry periods are calculated with the default Gamma distribution. In the light of all these findings, it can be emphasized that SPI drought estimation should be made through the theoretical probability distribution model that can best represent the data in accordance with the conditions of each studied region. This would be a factor in increasing the success of the decisions to be taken.

Data Availability

Data can be obtained through Turkish State Meteorological Service. The author is not authorized to supply the data. If one, but it can be obtained by personal application to the Turkish State Meteorological Service.

Conflicts of Interest

The authors declare that they have no conflicts of interest.

Authors' Contributions

Conceptualization was done by M.A.H.; methodology was done by M.A.H. and M.S.G.; writing-review and editing was done by M.A.H.; visualization was done by M.S.G.; and supervision was done by M.A.H.. All authors have read and agreed to the published version of the manuscript.

Acknowledgments

The authors thank the General Directorate of Meteorology for helping to provide the data used in this study.

References

[1] Ç. M. Akgul and I. Dino, "Climate change impact assessment in residential buildings utilizing RCP4.5 and RCP8.5 scenarios," *Journal of the Faculty of Engineering and Architecture of Gazi University*, vol. 35, pp. 3 1665–1683, 2020.

[2] M. E. Schlesinger, "Model projections of the climatic changes induced by increased atmospheric CO 2," in *Proceedings of the Symposium on Climate and Geo-Sciences*, Louvainla-Neuve, Belgium, August, 1988.

[3] G. J. McCabe and D. M. Wolock, "Detectability of the effects of a hypothetical temperature increase on the Thornthwaite moisture index," *Journal of Hydrology*, vol. 125, no. 1-2, pp. 25–35, 1991.

[4] Intergovernmental Panel on Climate Change (Ipcc), "Climate change 2007: the physical science basis," in *Contribution of Working Group I to the Fourth Assessment Report of the Intergovernmental Panel on Climate Change*, S. Solomon, D. Qin, M. Manning et al., Eds., Cambridge University Press, Cambridge, UK, 2007.

[5] P. H. Gleick, "Regional hydrologic consequences of increases in atmospheric CO2 and other trace gases," *Climatic Change*, vol. 10, no. 2, pp. 137–160, 1987.

[6] Intergovernmental Panel on Climate Change (Ipcc), "Climate change 2013: the physical science basis," in *Contribution of Working Group I to the Fifth Assessment Report of the Intergovernmental Panel on Climate Change*, T. F. Stocker, Ed., Cambridge University Press, Cambridge UK, 2013.

[7] G. Leng, Q. Tang, and S. Rayburg, "Climate change impacts on meteorological, agricultural and hydrological droughts in China," *Global and Planetary Change*, vol. 126, pp. 23–34, 2015.

[8] M. Jehanzaib and T. W. Kim, "Exploring the influence of climate change-induced drought propagation on wetlands," *Ecological Engineering*, vol. 149, Article ID 105799, 2020.

[9] J. Hougton, *Global Warming: The Complete Briefing*, Cambridge University Press, New York, NY, USA, Fourth edition, 2012.

[10] A. H. Sellers and K. McGuffie, *The Future of the Word's Climate*, Elsevier, New York, NY, USA, Second edition, 2012.

[11] E. Kapluhan, "Drought and drought in Turkey effect of agriculture," *Marmara Coğrafya Dergisi*, vol. 27, pp. 487–510, 2013.

[12] H. Tabari and P. Hosseinzadeh Talaee, "Moisture index for Iran: spatial and temporal analyses," *Global and Planetary Change*, vol. 100, pp. 11–19, 2013.

[13] G. Zhu, D. Qin, H. Tong et al., "Variation of thornthwaite moisture index in hengduan mountains, China," *Chinese Geographical Science*, vol. 26, no. 5, pp. 687–702, 2016.

[14] S. Mukherjee, A. Mishra, and K. Trenberth, "Climate change and drought: a perspective on drought indices," *Current Climate Change Reports*, vol. 4, no. 2, pp. 145–163, 2018.

[15] F. Giorgi, "Climate change hot-spots," *Geophysical Research Letters*, vol. 33, no. 8, Article ID L08707, 2006.

[16] X. Gao, J. S. Pal, and F. Giorgi, "Projected changes in mean and extreme precipitation over the Mediterranean region from a high resolution double nested RCM simulation," *Geophysical Research Letters*, vol. 33, no. 3, pp. 1–4, 2006.

[17] X. Gao and F. Giorgi, "Increased aridity in the Mediterranean region under greenhouse gas forcing estimated from high resolution simulations with a regional climate model," *Global and Planetary Change*, vol. 62, no. 3-4, pp. 195–209, 2008.

[18] O. L. Sen, A. Unal, D. Bozkurt, and T. Kindap, "Temporal changes in the Euphrates and Tigris discharges and teleconnections," *Environmental Research Letters*, vol. 6, no. 2, pp. 024012–024019, 2011.

[19] K. Yurekli, "Impact of climate variability on precipitation in the upper euphrates-tigris rivers basin of southeast Turkey," *Atmospheric Research*, vol. 154, pp. 25–38, 2015.

[20] M. Türkes, "Observed and projected climate change, drought and desertification in Turkey," *Ankara University Journal of Environmental Sciences*, vol. 4, no. 2, pp. 1–32, 2012.

[21] B. Önol and F. H M Semazzi, "Regionalization of climate change simulations over the eastern mediterranean," *Journal of Climate*, vol. 22, no. 8, pp. 1944–1961, 2009.

[22] A. Kitoh, A. Yatagai, and P. Alpert, "First super-high-resolution model projection that the ancient Fertile Crescent will disappear in this century," *Hydrological Research Letters*, vol. 2, no. 1–4, pp. 1–4, 2008.

[23] Y. Fujihara, K. Tanaka, T. Watanabe, T. Nagano, and T. Kojiri, "Assessing the impacts of climate change on the water resources of the Seyhan River Basin in Turkey: use of dynamically downscaled data for hydrologic simulations," *Journal of Hydrology*, vol. 353, no. 1-2, pp. 33–48, 2008.

[24] E. Kahya and S. Kalayci, "Trend analysis of streamflow in Turkey," *Journal of Hydrology*, vol. 289, no. 1-4, pp. 128–144, 2004.

[25] K. Yurekli, "Scrutinizing variability in full and partial rainfall time series by different approaches," *Natural Hazards*, vol. 105, no. 3, pp. 2523–2542, 2021.

[26] E. Atış, "Agriculture and Environment," in *Agriculture in Turkey*, F. Yavuz, Ed., pp. 161–176, Ministry of Agriculture and Rural Affairs, Ankara,Turkey, 2005.

[27] B. Cakmak, I. H. O. Unver, and T. Akuzum, "Agricultural water use in Turkey," *Water International*, vol. 29, no. 2, pp. 257–264, 2004.

[28] I. Cicek and M. Ataol, "A new approach for determining the water potential of Turkey," *Turkish Journal of Geographical Sciences*, vol. 7, no. 1, pp. 51–64, 2009.

[29] G. Wang, "Agricultural drought in a future climate: results from 15 global climate models" participating in the IPCC 4th assessment," *Climate Dynamics*, vol. 25, no. 7–8, pp. 739–753, 2005.

[30] T. B. McKee, N. J. Doesken, and J. Kleist, "The relationship of drought frequency and duration to time scale," in *Proceedings of the Eighth Conference On Applied Climatology*, pp. 179–184, American Meteorological Society, Anaheim, CA, USA, January, 1993.

[31] World Meteorological Organization, *Standardized Precipitation Index User Guide*, World Meteorological Organization, WMO-1090, Switzerland, 2012.

[32] F. Sienz, O. Bothe, and K. Fraedrich, "Monitoring and quantifying future climate projections of dryness and wetness extremes: SPI bias," *Hydrology and Earth System Sciences*, vol. 16, no. 7, pp. 2143–2157, 2012.

[33] N. B. Guttman, "On the sensitivity of sample L moments to sample size," *Journal of Climate*, vol. 7, no. 6, pp. 1026–1029, 1994.

[34] N. B. Guttman, "Accepting the standardized precipitation index: a calculation algorithm," *JAWRA Journal of the American Water Resources Association*, vol. 35, no. 2, pp. 311–322, 1999.

[35] D. C. Edwards, *Characterıstıcs of 20th century Drought in the Unıted States at Multiple Time Scales, Master Thesis*, Colorado State University, Fort Collins, CA, USA, 1997.

[36] H. C. S. Thom, "Some methods of climatological analysis," WMO Technical Note Number 81, p. 53, Secretariat of the World Meteorological Organization, Geneva, Switzerland, 1966.

[37] G. C. Blain, A. M. H. de Avila, and V. R. Pereira, "Using the normality assumption to calculate probability-based standardized drought indices: selection criteria with emphases on typical events," *International Journal of Climatology*, vol. 38, pp. 418–436, 2018.

[38] G. Guenang, M. Komkoua, M. Pokam et al., "Sensitivity of SPI to distribution functions and correlation between its values at different time scales in central Africa," *Earth Systems and Environment*, vol. 3, pp. 1–12, 2019.

[39] J. H. Stagge, L. M. Tallaksen, L. Gudmundsson, A. F. Van Loon, and K. Stahl, "Candidate distributions for climatological drought indices (SPI and SPEI)," *International Journal of Climatology*, vol. 35, no. 13, pp. 4027–4040, 2015.

[40] G. C. Blain and M. C. Meschiatti, "Inadequacy of the gamma distribution to calculate the standardized precipitation index," *Revista Brasileira de Engenharia Agrícola e Ambiental*, vol. 19, no. 12, pp. 1129–1135, 2015.

[41] M. Yılmaz, H. Alp, F. Tosunoglu, Ö. L. Aşıkoğlu, and E. Eriş, "Impact of climate change on meteorological and hydrological

droughts for Upper Coruh Basin, Turkey," *Natural Hazards*, vol. 112, no. 2, pp. 1039–1063, 2022.

[42] P. Mahmoudi, A. Ghaemi, A. Rigi, and S. M. Amir Jahanshahi, "Retracted article: recommendations for modifying the standardized precipitation index (SPI) for drought monitoring in arid and semi-arid regions," *Water Resources Management*, vol. 35, no. 10, pp. 3253–3275, 2021.

[43] P. Pieper, A. Düsterhus, and J. Baehr, "A universal Standardized Precipitation Index candidate distribution function for observations and simulations," *Hydrology and Earth System Sciences*, vol. 24, no. 9, pp. 4541–4565, 2020.

[44] A. B. Hezarani, U. Zeybekoglu, and A. U. Keskin, "Hydrological and meteorological drought forecasting for the Yesilirmak river basin, Turkey," *Journal of Sustainable Engineering Applications and Technological Developments*, vol. 4, no. 2, pp. 121–135, 2021.

[45] S. Doğan, *Spatio-Temporal Analysis of Drought Characterization in Konya Closed Basin*, Ph.D. Thesis, p. 107, The Graduate School of Natural and Applied Science of Selçuk University, Konya, 2013.

[46] J. T. Shiau, "Effects of gamma-distribution variations on SPI-based stationary and nonstationary drought analyses," *Water Resources Management*, vol. 34, no. 6, pp. 2081–2095, 2020.

[47] N. Seckin, R. Yurtal, T. Haktanir, and A. Dogan, "Comparison of probability weighted moments and maximum likelihood methods used in flood frequency analysis for Ceyhan river basin," *Arabian Journal for Science and Engineering*, vol. 35, pp. 49–69, 2010.

[48] A. R. Rao and K. H. Hamed, *Flood Frequency Analysis*, CRC Publications, New York, NY, USA, 2000.

[49] J. N. Okpara, E. A. Afiesimama, A. C. Anuforom et al., "The applicability of standardized precipitation index: drought characterization for early warning system and weather index insurance in West Africa," *Natural Hazards*, vol. 89, no. 2, pp. 555–583, 2017.

[50] G. C. Blain, A. M. H. de Avila, and V. R. Pereira, "Using the normality assumption to calculate probability-based standardized drought indices: selection criteria with emphases on typical events," *International Journal of Climatology*, vol. 38, pp. e418–e436, 2018.

[51] R. Zhao, H. Wang, C. Zhan, S. Hu, M. Ma, and Y. Dong, "Comparative analysis of probability distributions for the Standardized Precipitation Index and drought evolution in China during 1961–2015," *Theoretical and Applied Climatology*, vol. 139, no. 3-4, pp. 1363–1377, 2020.

[52] W. Wang, L. Qiu, R. Sa, S. Dang, F. Liu, and X. Xiao, "Effect of socioeconomic characteristics and lifestyle on BMI distribution in the Chinese population: a population-based cross-sectional study," *BMC Public Health*, vol. 21, no. 1, pp. 1369–1383, 2021.

[53] U. A. Kömüşçü, A. Erkan A, E. Turgu, and K. F. Sönmez, "A new insight into drought vulnerability in Turkey using the standard precipitation index," *Journal of Environmental Hydrology*, vol. 12, no. 18, 2004.

[54] K. Sonmez, A. Ü. Kömüscü, A. Erkan, and E. Turgu, "An analysis of spatial and temporal dimension of drought vulnerability in Turkey using the standardized precipitation index," *Natural Hazards*, vol. 35, no. 2, pp. 243–264, 2005.

[55] G. Akturk, U. Zeybekoglu, and O. Yildiz, "Assessment of meteorological drought analysis in the Kizilirmak river basin, Turkey," *Arabian Journal of Geosciences*, vol. 15, no. 9, p. 850, 2022.